JOURNAL OF CATALYSIS 42, 408–417 (1976)

Comparison of Some Models of Porous Media in the Catalytic *para–ortho*-Hydrogen Conversion

L. DVOŘÁK AND P. SCHNEIDER

Institute of Chemical Process Fundamentals, Czechoslovak Academy of Sciences, 165 02 Prague-Suchdol, Czechoslovakia

Received July 22, 1975

The influence of intraparticle diffusion on the rate of the catalytic *para–ortho*-hydrogen conversion was experimentally studied at room temperature and total pressure from 200 to 760 Torr. The experimental effectiveness factors η_{exp} were determined for five sizes of catalyst pellets and compared with the predictions (η_{pred}) based on 16 models of porous media divided into four groups: (A) non-catalytic models, (B) models without an adjustable parameter, (C) models with one, and (D) with two adjustable parameters. The evaluation of models was based on differences between η_{exp} and η_{pred} and on constancy and acceptability of adjustable parameters. Group A yields unsatisfactory values of η_{pred}. In group B, models which take into account transition diffusion, the best results were obtained with the multidisperse model of Cunningham and Geankoplis (*Ind. Eng. Chem. Fundam.* **7**, 535 (1968)). The best model from group C is the parallel pore model of Johnson and Stewart (*J. Catal.* **4**, 248 (1965)). For the experimental conditions used the two-parameter semi-linked pore model degenerated into the parallel pore model.

NOMENCLATURE

c	total molal hydrogen concentration
d	relative difference between η_{pred} and η_{exp}
D	effective diffusivity
$\mathfrak{D}(r)$	diffusivity in transition region
$\mathfrak{D}_{AB}$	binary bulk diffusivity
$\mathfrak{D}_{AK}$	Knudsen diffusivity in a capillary
$f(r)$	frequency function of pore size distribution, $f=(1/V_T)(dV/d\log r)$
k, k'	rate constants
K_A	adsorption coefficient
L	pellet length
M	Thiele modulus
M_A	molecular weight of component A
p	gas pressure
R	reaction rate
R_g	gas constant
r	capillary (pore) radius
$\bar{r}$	average pore radius
S	specific surface
s	relative standard deviation
T	absolute temperature (K)
V, V_T	pore volume in pores with radius less than r, and total pore volume, respectively
v_A	mean thermal velocity of molecules A
y, y_e	mole fraction of $p-H_2$ in reacting mixture, and at equilibrium, respectively
η	effectiveness factor
δ	mean value of $\lvert d \rvert$
Δ	distributivity
ρ	apparent pellet density
ϵ	porosity

Subscripts, superscripts

exp	for experimental value
pred	for calculated value

i	for small mesopores
a, j, k	for large mesopores or macropores
o	for powder (without superscript, for pellet)
isol	for isolated pore model
parall	for parallel pore model
rem	most remote value, still in the 95% confidence region
opt	optimum value

INTRODUCTION

In order to predict the effect of mass and heat diffusion inside porous catalysts on the rate of a catalytic reaction it is necessary to start with a model of porous structure. Such a model can be presented in various forms.

(i) One possibility is to select a pore unit which is so simple that mass transfer inside it can be described quantitatively; then, a regular arrangement of these units has to be supposed, such that (at least some) textural properties of the catalyst, e.g., pore volume, pore size distribution, etc., are identical with properties of the substituted model porous medium. The catalyst effectiveness can then be predicted by solving the mass (and heat) balances of this substituted model medium. Usually, values of some textural parameters of the model porous medium have to be obtained by fitting experimentally obtained reaction rates to predicted ones or by evaluation of other carefully selected independent experiments (diffusion without catalytic reaction, permeation of pure gases, etc.).

(ii) Another approach starts in the same way, but in this case the development is aimed towards the formulation of effective diffusion coefficients. Using these coefficients and the Fick Law the catalyst effectiveness can be expressed as if the porous medium would be homogeneous. In some cases adjustable parameters are introduced in the same way as in (i).

It is the aim of this paper to compare different models of porous media proposed in the literature, using experimentally obtained values of catalyst effectiveness. Because the character of the catalytic reaction as well as the nature and number of reaction components are reflected in the predictions, we have chosen the simplest possible reaction, viz., the *para–ortho*-hydrogen conversion at 25°C, catalyzed by the commercial Girdler G-13 catalyst.

The rate of *para*-hydrogen conversion is of first order in *para*-hydrogen surface concentration; thus the simple Langmuir–Hinshelwood rate equation can be used. This equation is further simplified because of the chemical identity of *para*- and *ortho*-hydrogen species. Thus

$$R = kK_A c(y - y_e)/(1 + K_A c), \quad (1)$$

where k is the rate constant, K_A the adsorption equilibrium constant of hydrogen, and c is the total molal hydrogen concentration; y and y_e denote the mole fraction of *para*-hydrogen in the reacting mixture and in chemical equilibrium ($y_e(25°C) = 0.25$[1]). At constant hydrogen pressure Eq. (1) simplifies to

$$R = k'(y - y_e), \quad (2)$$

where $k' = k'(c)$. The kinetics of this reaction free of transport effects were studied on powdered catalyst in an integral fixed bed reactor at six hydrogen pressure levels (200–760 Torr).

Experiments with intraparticle diffusion intrusion were carried out on large cylindrical catalyst pellets with all but one circular front face sealed. Thus the geometry of an infinite slab was realized; five pellets of identical apparent density and variable lengths (1.0–4.5 cm) were used as well as three pellets with the same length (1.5 cm) and changing apparent density (1.95–2.26 g/cm^3). In these cases the ideally mixed flow catalytic reactor with external recirculation was employed and the conversion rates were obtained at hydrogen pressures from 200 to 760 Torr.

THE MODELS USED

The models[1] summarized in Table 1 were separated into four groups (A, B, C, D), the main criterion being the number of adjustable parameters which appear in the model. The first group, *the noncatalytic models* (*A*) includes older models which were developed for description of diffusion without catalytic reaction in porous solids. These models predict the effective diffusion coefficient D from the known porosity of the porous solid (ϵ) and binary diffusivity of the diffusing gases ($\mathfrak{D}_{AB}$) without any adjustable parameter. The influence of intraparticle diffusion on the rate of catalytic reaction can be expressed by means of the effectiveness factor η defined in the usual way. For the first order isothermal reaction taking place in pseudohomogenous porous catalyst with an infinite slab geometry, characterized by effective diffusivity D, η is predicted by

$$\eta = \tanh(M)/M, \tag{3}$$

where M is the Thiele modulus (*4*),

$$M^2 = L^2k'/(cD) \tag{4}$$

[L is the half depth of the infinite slab, i.e., the length of the catalyst pellet used, and the rate constant k' is expressed per unit volume of the pellet (mol/cm^{3}s)].

The second group, *no parameter models* (*B*), summarizes models developed intentionally for prediction of effectiveness factors. The textural characteristics required for calculation of effective diffusivity, D, include average pore radii and corresponding fractions of pore volume. Similar to group A, no adjustable parameter is involved, and η is calculated from Eqs. (3) and (4).

One parameter models (*C*) include models which predict η using Eqs. (3) and (4) with the effective diffusivity calculated using a frequency function of pore size distribution [$f(r)$]. Into this group also falls the isolated pore model for which η is obtained by integrating effectiveness factors of isolated pores (cf. Table 1). The adjustable parameter of these models, tortuosity q, can be interpreted as a measure of the increased diffusion path length due to irregular directions of the pores. Because the real porous structure is greatly simplified, other textural factors, e.g., pore constrictions, varying pore diameter, pore roughness, etc., enter tortuosity, too.

The semi-linked pore model belongs to the group of *two-parameter models* (*D*). In this model part of the pores (Δ) is mutually isolated; in the remaining part ($1 - \Delta$) complete mixing between the pore contents is assumed. The isolated pore model and parallel pore model [Johnson–Stewart (*13*, *14*)] from group C represent limiting cases ($\Delta = 0$ or $\Delta = 1$) of this more general model. Besides distributivity Δ, tortuosity q represents the adjustable parameter. For the first-order reaction the effectiveness factor can be easily expressed as

$$\eta = \Delta\eta_{isol} + (1 - \Delta)\eta_{parall}, \tag{5}$$

where η_{isol} and η_{parall} are effectiveness factors calculated according to isolated pore and parallel pore models.

EXPERIMENTAL

Steady-state reaction rates on powdered catalyst (0.4-mm diameter) were measured in an integral flow reactor (8-mm i.d., bed length 50 mm). For measurements with catalyst pellets, a continuous stirred reactor with recirculation (magnetically operated two-stroke piston pump) was used. The hydrogen stream after purification was split into two branches: In the stream which served as standard in the reference cell of the thermal conductivity detector (TCD) the ratio o-H_2/p-$H_2 = 3/1$ was maintained by equilibrating hydrogen on a sufficient amount of active Ni catalyst at

[1] The names of models are assigned rather arbitrarily: usually the authors' names are used. A descriptive title is used alternatively in few cases.

TABLE 1

Compared Models of Porous Media

Group	Model name	Expression for D or η[a]
A	Maxwell (*2*)	$D = \mathfrak{D}_{AB} 2\epsilon/(3 - \epsilon)$
	Buckingham (*3*)	$D = \mathfrak{D}_{AB}\epsilon^2$
	Dumanski (*4*)	$D = \mathfrak{D}_{AB}[1 - (1 - \epsilon)^{\frac{1}{2}}]$
	Bruggemann (*5*)	$D = \mathfrak{D}_{AB}\epsilon^{\frac{3}{2}}$
	Hugo and Paratella (*6*)	$D = \mathfrak{D}_{AB} t^2(2 - t)/(2 - 3t + 2t^2)$; $\epsilon = 3t^2 - 2t^3$
	Masamune and Smith (*7*)	$D = \mathfrak{D}_{AB}\epsilon/(4 - 3\epsilon)$
B	Wheeler (*8*)[b]	$D = \mathfrak{D}_{AB}(\epsilon/\sqrt{2})[1 - \exp(-\mathfrak{D}_{AK}(\bar{r})/\mathfrak{D}_{AB})]$
	Weisz and Schwartz (*9*) (spherical pore model)[b]	$D = (\epsilon^2/\sqrt{3})/[1/\mathfrak{D}_{AB} + 2/(3\mathfrak{D}_{AK}(\bar{r}))]$
	Wakao and Smith (*10*) (random pore model)[c,d]	$D = \epsilon_a^2[1/\mathfrak{D}_{AB} + 1/\mathfrak{D}_{AK}(\bar{r}_a)]^{-1} + [(1 + 3\epsilon_a)/(1 - \epsilon_a)]\epsilon_i^2\mathfrak{D}_{AK}(\bar{r}_i)\eta_i$
	Cunningham and Geankoplis (*11*) (multidisperse pore model)[c,d]	$D = 2\Sigma\epsilon_k\Sigma\epsilon_j[2/\mathfrak{D}_{AB} + 1/\mathfrak{D}_{AK}(\bar{r}_k) + 1/\mathfrak{D}_{AK}(\bar{r}_j)]^{-1} + [(1 + 3\epsilon_a)/(1 - \epsilon_a)]\epsilon_i^2\mathfrak{D}_{AK}(\bar{r}_i)\eta_i$
	Balfanz (*12*) (macropore model)[e,f]	$D = \epsilon(V_a S^0/V_a{}^0 S)^2 \int \mathfrak{D}(r) f(r) dr$
C	Johnson and Stewart (*13, 14*) (parallel pore model)[e,f]	$D = (\epsilon/q^2) \int \mathfrak{D}(r) f(r) dr$
	Rothfeld (*15*) (mean pore model)	$D = (\epsilon/q^2)[1/\mathfrak{D}_{AB} + 1/\mathfrak{D}_{AK}(\bar{r}_a)]$
	Nicholson and Petropoulos (*16*) (pore-in-series model)[e,f]	$D = (\epsilon/q^2)[\int f(r) dr/r^2]^2/[\int f(r) dr/r^4\mathfrak{D}(r)]$
	Wakao (*17, 18*)[b,e,f]	$D = (\epsilon/q^2)[\int (\mathfrak{D}(r)/r)^{\frac{1}{2}} f(r) dr]^2\bar{r}$
	Isolated pore model (*19*)[b,e,f]	$\eta = \bar{r}\int \eta(r) f(r) dr/r$; $\eta(r) = \tanh[M(r)]/M(r)$; $M(r) = Lq[k\bar{r}/\epsilon c r\mathfrak{D}(r)]^{\frac{1}{2}}$
D	Semi-linked pore model (*19*)	$\eta = \Delta\eta_{isol} + (1 - \Delta)\eta_{parall}$

[a] η is given by Eqs. (*3*) and (*4*).
[b] $\bar{r} = [\int f(r) dr/r]^{-1}$.
[c] $\bar{r} = \int r f(r) dr$.
[d] $\eta_i = 1$.
[e] $\mathfrak{D}(r) = [1/\mathfrak{D}_{AB} + 1/\mathfrak{D}_{AK}(r)]^{-1}$.
[f] Integration limits: $r = 0$; $r \to \infty$.

25°C. In the second branch, hydrogen was equilibrated on the Ni catalyst at liquid nitrogen temperature; the resulting stream, with o-H_2/p-$H_2 = 1/1$, was fed into the catalytic reactor. Part of the hydrogen stream leaving the reactor was analyzed in TCD. Constant pressure was adjusted by needle valves and a solenoid valve activated by a contact manometer.

The powdered Girdler G-13 catalyst ($CuO \cdot Cr_2O_3$) and the pellets prepared from the catalyst powder in a hydraulic press were reduced prior to kinetic runs in a hydrogen stream for 84 hr. The pore size distribution was determined by a combination of mercury porosimetry and evaluation of the desorption branch of a benzene adsorption isotherm (*20*). Porosities of pellets were determined from true (4.53 g/cm³) and apparent densities measured pycnometrically with helium and mercury. The pore size distribution curves of all pellets

exhibited high maxima at pore radii about 20 and 200 Å and a nonzero tail up to 75,000 Å; for less dense pellets (2.00 and 1.95 g/cm³) a third low maximum appeared at about 20,000 Å.

The absence of intraparticle and external diffusion in runs with powdered catalyst was verified experimentally. The piston character of gas flow in the reactor was checked using Mear's criterion (*21*). Conditions for absence of external diffusion and ideal mixing for pellet runs were established by changing the circulation rate of the piston pump.

RESULTS

Kinetic runs on powdered catalyst confirmed the first-order rate equation (2) at each of the six constant hydrogen pressure levels. From the pressure dependence of the experimental rate constants, the constants of Eq. (1) were determined: $k(25°C) = 3.5 \times 10^{-4}$ mol/cm³ s $= 1.57 \times 10^{-4}$ mol/g s, $K_A(25°C) = 4.3 \times 10^4$ cm³/mol ($\doteq 1.75$ atm^{-1}). As expected the first-order rate behavior was retained even in the pellet runs at constant hydrogen pressure. Thus the experimental values of effectiveness factors η_{exp} were calculated as ratios of rate constants for pellet and powder runs at the same hydrogen pressure. Effectiveness factors changed from about 0.01 (long pellets, high hydrogen pressure) to 0.1 (short pellets, low pressure).

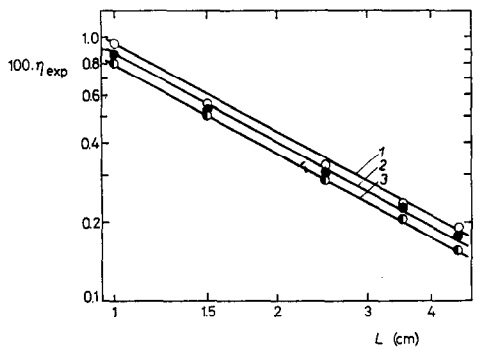

FIG. 1. Experimental effectiveness factors for pellets with different lengths. Pellet density, 2.26 g/cm³; hydrogen pressure: (*1*), 200 Torr; (*2*), 500 Torr; (*3*), 760 Torr.

The practically inverse proportionality of η_{exp} on pellet length (Fig. 1) indicates that the *para–ortho*-hydrogen conversion takes place in the region of strong influence of intraparticle diffusion. In this region, the porous medium can be considered as semiinfinite and the tanh (M) term in the expressions for η limits to one; thus $\eta \sim 1/M \sim 1/L$.

The slight increase of η with decreasing hydrogen pressure (Fig. 1) reflects the pressure dependence of the diffusion coefficient.

For models which obey Eqs. (2) and (3) experimental values of effective diffusivity D_{exp} can be obtained from experimental η's. It is apparent from Table 2 that D_{exp} increases with hydrogen pressure decrease, as expected. Higher diffusivities for less dense pellets can be explained as a consequence of increased average pore radius. Contrary to expectations, D_{exp} varies also with pellet length L; this indicates that models leading to Eqs. (2) and (3) are oversimplified and are not able, therefore, to describe the reaction-diffusion problem completely.

The pressure dependence of effective diffusivities can be used for characterization of the diffusion region in which the conversion reaction takes place. If we assume (as, for example, in the Weisz–Schwartz (*9*) and Rothfeld (*15*) models) that

$$D^{-1} = D_{AK}^{-1} + D_{AA}^{-1} \qquad (6)$$

(D_{AK} is the pressure-independent effective Knudsen diffusion coefficient, D_{AA} is the effective bulk self-diffusion coefficient of hydrogen [$D_{AA} \sim 1/P$], the plot of D_{exp}^{-1} vs P should yield a straight line. This is verified in Fig. 2, from which contributions of bulk and Knudsen diffusion are apparent. Obviously, at all hydrogen pressure levels used, neither pure Knudsen nor pure bulk diffusion operates.

TABLE 2

Experimental Effective Diffusivities [a]

Density (g/cm³)	Pellet length (cm)	Hydrogen pressure (Torr)					
		200	300	400	500	600	760
2.26	1.0	8.52[a]	5.51	5.34	4.50	3.60	3.28
2.26	1.5	6.81	4.83	4.62	3.98	3.43	3.19
2.26	2.5	6.39	4.55	4.21	3.72	3.26	2.76
2.26	3.5	6.71	4.58	4.28	3.84	3.37	2.61
2.26	4.5	6.81	3.45	3.38	3.64	3.05	2.34
2.00	1.5	14.41	10.03	9.49	7.20	8.05	6.43
1.95	1.5	14.49	11.97	9.63	9.24	8.71	6.73

[a] Values are $100 \cdot D_{exp}(cm^2/s)$.

Models from groups A and B predict effectiveness factors without the necessity of any adjustable parameter. (Molecular diffusivities $\mathfrak{D}_{HH}$ necessary for these calculations were obtained from the Hirschfelder, Curtiss, and Bird equation (*22*), and the Knudsen diffusivities $\mathfrak{D}_{KH}$ from $\mathfrak{D}_{KA} = (\frac{2}{3})(8R_gT/\pi M_A)^{\frac{1}{2}}$). These models can thus be compared using the differences between predicted and experimental η's. Table 3 summarizes averages δ of absolute values of relative differences $|d|$ between η_{pred} and η_{exp}: $d = (\eta_{pred} - \eta_{exp})/\eta_{exp}$. The averaging was made over six hydrogen pressure levels (200–760 Torr), five pellet lengths (1–4.5 cm) with pellet density 2.26 g/cm³, and two pellet densities (1.95 and 2.00 g/cm³) with length 1.5 cm (42 values in total). Relative standard deviations of means, s, are also included.

The δ values show that the models A give quite unsatisfactory predictions of effectiveness factors. This is understandable because these models consider bulk diffusion only, whereas diffusion actually takes place in the transition region. The models B which take this fact into account are better by an order of magnitude. In this group the predicted η's were usually higher than the experimental ones, with the exception of the Wheeler and Weisz–Schwartz pore models. The success of the tri- and tetra-disperse pore models of Cunningham and Geankoplis follows from the fact that these models account for the actual pore structure more thoroughly than other models.

One of the possibilities of comparing the one-parameter models (C) consists of analyzing the adjustable parameter tortuosity, q. According to the simple physical interpretation tortuosity should be higher than unity. However, because in addition to the increased diffusion path length, other phenomena may affect q, the condition $q \geqslant 1$ must not be considered as quite strict. Probably more emphasis ought to be given to constancy of q; experiments performed under different conditions should yield the same tortuosity.

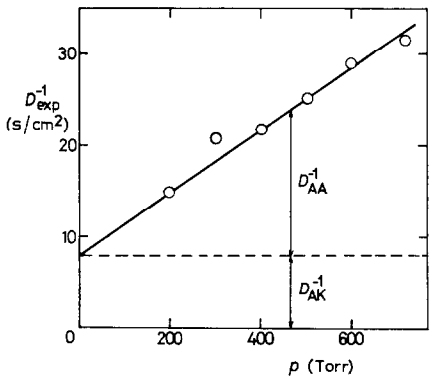

FIG. 2. Pressure dependence of D_{exp}^{-1}. Pellet density, 2.26 g/cm³; pellet length, 1.5 cm.

TABLE 3

Relative Differences (δ) between η_{pred} and η_{exp} and Their Relative Standard Deviations (s)

Models	δ (%)	s (%)	Models	δ (%)	s (%)
Models A			Models B		
Maxwell	397	14	Wheeler	28	2
Buckingham	299	10	Weisz, Schwartz (spherical pore model)	43	1
Dumanski	244	9			
Bruggeman	369	13	Wakao, Smith (random pore model)	78	2
Hugo, Paratella[a]	140	7			
Hugo, Paratella[a]	383	13	Cunningham, Geankoplis (tridisperse pore model)	12	1
Hugo, Paratella[a]	553	20			
			Cunningham, Geankoplis (tetradisperse pore model)	13	1
			Cunningham, Geankoplis (pentadisperse pore model)	17	1
			Balfanz (macropore model)	76	2
Models C			Models D		
Johnson, Stewart (parallel pore model)	5	1	Semi-Linked pore model	6	1
Rothfeld (mean pore model)	10	1			
Nicholson, Petropoulos (pore-in-series model)	11	1			
Wakao	10	1			
Isolated pore model	11	1			

[a] For three roots of cubic equation in t (see Table 1).

Tortuosities for different C models were computed from the respective equations predicting effectiveness factors so that $\eta_{exp} = \eta_{pred}$. Thus for each set of conditions (hydrogen pressure, pellet length, and density) a corresponding q resulted. In Table 4 the averaged values of q are given for three pellets differing in density. (For

TABLE 4

Mean Tortuosities (q) and Their Relative Standard Deviations (s) for One-Parameter Models

Model	Pellet density (g/cm³)					
	2.26		2.00		1.95	
	q	s (%)	q	s (%)	q	s (%)
Johnson, Stewart (parallel pore model)	2.04	2.0	1.81	1.7	1.91	1.0
Rothfeld (mean pore model)	1.52	2.6	1.16	5.2	1.09	4.6
Nicholson, Petropoulos (pores-in-series model)	0.23	4.3	0.15	6.7	0.14	7.1
Wakao	0.85	2.4	0.65	4.6	0.62	3.2
Isolated pore model	0.83	2.4	0.59	5.1	0.56	5.4

the pellets with highest density, the averaging was made over all hydrogen pressure levels as well as over all pellet lengths; for the two low density pellets averaging is only over hydrogen pressure levels.) The requirement $q \gtrless 1$ is met only by the parallel pore and the Rothfeld models. Constancy of q is characterized in the same table by relative standard deviations, s, of the mean values. It is obvious that the best constancy of tortuosity is obtained from the parallel pore model (which also satisfies the $q \gtrless 1$ condition). In the second place are the Rothfeld model, for which $q \gtrless 1$ is also valid, and the Wakao and the isolated pore models, where q is slightly less than unity. If the requirement $q \gtrless 1$ is weakened, the isolated pore model and the Wakao model appear also as plausible. The pores-in-series model exhibits the highest variation of tortuosity, which is, moreover, too low. This is probably because this model was originally developed for microporous media in which diffusion is of the Knudsen type.

Variation of tortuosity with pellet length and hydrogen pressure can be followed also directly. In Fig. 3 the $q(p)$ dependence for pellets with density 2.26 g/cm³ and the parallel pore and the Rothfeld models is plotted for illustration. The systematic increase of q with hydrogen pressure for the Rothfeld model is obvious in comparison with the parallel pore model. From statistical evaluation (analysis of variance) it follows that the pressure dependence of tortuosity is nearly within the limits of experimental error for the parallel pore model only. For other models from group C, the change of tortuosity with hydrogen pressure and pellet length is statistically significant.

In order to compare the one-parameter models C with the parameterless models A and B, the average deviations, δ, between the experimental effectiveness factor and effectiveness factors predicted with q values from Table 4 were calculated (Table 3). One-parameter models predict effectiveness

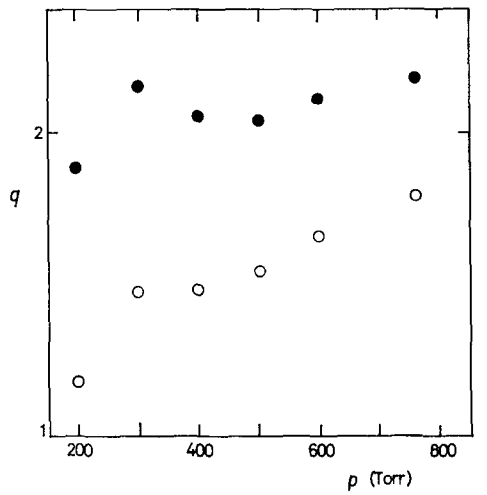

FIG. 3. Tortuosities for the parallel pore (●) and the Rothfeld (○) models. Pellet density, 2.26 g/cm³; values of q are averages over five pellet lengths (1–4.5 cm).

factors on average within 5–10% of η_{exp}; even in this respect the parallel pore model shows its superiority ($\delta = 5\%$).

Adjustable parameters of the only representative of two-parameter models (group D), the semi-linked pore model, were evaluated numerically; the grid search method with constraints $[q > 0, \Delta \in (0, 1)]$ were used to minimize the sum of squared deviations between experimental and predicted η's. The obtained pairs of optimum parameters q^{opt} and Δ^{opt} are summarized in Table 5. Parameters q and Δ are correlated

TABLE 5

Semi-Linked Pore Model[a]

Pellet density (g/cm³)	Length (cm)	q^{opt}	Δ^{opt}	q^{rem}	Δ^{rem}
2.26	1.0–4.5	1.96	0.0	1.66	0.26
2.26	1.5	2.02	0.0	1.42	0.50
2.00	1.5	1.81	0.0	1.00	0.67
1.95	1.5	1.38	0.4	1.94	0.00
				0.99	0.68

[a] Optimum (q^{opt}, Δ^{opt}) and most remote pairs of q and Δ corresponding to 95% confidence level (q^{rem}, Δ^{rem}).

and hence in the plane q–Δ a region exists within which all combinations of q and Δ lead to the values of optimized function which are on 95% probability level indistinguishable from the minimum value (corresponding to q^{opt} and Δ^{opt}). These regions are characterized in Table 5 by pairs of q^{rem} and Δ^{rem}, which are most remote from the optimum pairs but still within the 95% confidence region.

It follows from this table that in all cases tortuosities are higher than unity, including the most remote values q^{rem}. Optimum distributivities for denser pellets (2.26 and 2.0 g/cm³) are zero; this corresponds to one of the limiting types of this model, viz., the parallel pore model in which all pores are interconnected so that mixing between their contents takes place. (The slight difference between q^{opt} and tortuosities for the parallel pore model is due to differences in optimization criteria). Only for the least dense pellet (1.95 g/cm³) $\Delta = 0.4$, which indicates that part of the pore volume (40%) is formed by pores which are mutually isolated. Some mutually isolated pores may, however, be present also in the denser pellets; this is testified to by nonzero values of Δ^{rem}. If the adjustable parameter Δ has only the simple physical meaning (i.e., fraction of volume of pores which are mutually isolated), then one would expect increase of this parameter with pellet density (increased compressing pressure would probably result in blocking of pore interconnections). This is, however, not the case. Thus, similar to tortuosity, distributivity has to be considered as a more complex parameter, with a not easily definable physical meaning.

In order to compare the semi-linked pore model with other models, differences between experimental effectiveness factors and effectiveness factors predicted by this model (using q^{opt} and Δ^{opt}) were calculated. The average δ of absolute values of relative differences amounts to 6% (cf. Table 3), i.e., the prediction efficiency of this model is the same as for the parallel pore model. Because of degeneration of the semi-linked pore model into the parallel pore model in the studied case, no other result could have been, in fact, expected.

From the comparison of models based on average relative deviations between η_{exp} and $\eta_{pred} - \delta$ (Table 3), it follows that these deviations diminish in the order A, B, C, D. For reasons shown above the best model from group C (parallel pore model) gives the same results as the semi-linked pore model.

Deviations between η_{exp} and η_{pred} also depend on conditions (hydrogen pressure, pellet length, and density) for which this comparison is made. These deviations were analyzed statistically (analysis of variance) in order to show what variables in what models affect the agreement $\eta_{exp} - \eta_{pred}$ significantly and systematically. It appears that the effect of pellet length is significant at a similar level in all models used. The effect of pellet density is most significant for models from group A; in group B it is less marked but still significant. In groups C and D the influence of pellet density is practically insignificant. In this respect it is, however, necessary to add that the range of densities on which these results are based was rather limited. The effect of hydrogen pressure on $\eta_{exp} - \eta_{pred}$ deviations is the greatest for the models A. This effect is less but still significant for the models B and C. Only for the parallel pore model (C) and the semi-linked pore model (D) does the pressure dependence cease to be systematically significant.

REFERENCES

1. Fraunfeld, R., and Heimich, F., *Helv. Chim. Acta* **38**, 279 (1965).
2. Maxwell, C., "Treatise on Electricity and Magnetism I." Oxford University Press, Oxford, 1955.
3. Buckingham, E., Bull. No. 25, U. S. Dept. of Agriculture, Bureau of Soils, 1904.

4. Dumanski, A., *Kolloid Z.* **3**, 210 (1908).
5. Bruggemann, D. A. C., *Ann. Physik V* **24**, 636 (1935).
6. Hugo, P., and Paratella, A., *in* Simposio di Dinamica delle Reazzioni Chimiche, Padua, 1966.
7. Masamune, S., and Smith, J. M., *Amer. Inst. Chem. Eng. J.* **8**, 217 (1962).
8. Wheeler, A., *Advan. Catal.* **3**, 252 (1951).
9. Weisz, P. B., and Schwartz, A. B., *J. Catal.* **1**, 399 (1962).
10. Wakao, N., and Smith, J. M., *Ind. Eng. Chem. Fundam.* **3**, 127 (1964).
11. Cunningham, R. S., and Geankoplis, G. J., *Ind. Eng. Chem. Fundam.* **7**, 535 (1968).
12. Balfanz, F., PhD Dissertation. Humboldt University, Berlin, 1972.
13. Johnson, M. L. F., and Stewart, W. E., *J. Catal.* **4**, 248 (1965).
14. Satterfield, C. N., and Cadle, P. J., *Ind. Eng. Chem. Proc. Des. Develop.* **7**, 256 (1968).
15. Rothfeld, L. B., *Amer. Inst. Chem. Eng. J.* **9**, 19 (1963).
16. Nicholson, D., and Petropoulos, J. H., *Brit. J. Appl. Phys.* **1**, 1379 (1968).
17. Wakao, N., *Bull. Fac. Eng. Yokohama Nat. Univ.* **16**, 101 (1967).
18. Wakao, N., and Funaki, T., *Kagaku Kogaku* **31**, 485 (1967).
19. Dvořák, L., and Schneider, P., *Collect. Czech. Chem. Commun.*, in press.
20. Roberts, B. F., *J. Colloid Interface Sci.* **23**, 266 (1967).
21. Mears, D. E., *Ind. Eng. Chem. Proc. Des. Develop.* **10**, 541 (1971).
22. Bird, R. B., Steward, W. E., and Lightfoot, E. N., "Transport Phenomena." Wiley, New York, 1960.